electronics

MDPI

Article

A Communication Framework for Image Transmission through LPWAN Technology

Fabián Chaparro B. [1,*,†], Manuel Pérez [2,†] and Diego Mendez [2,†]

[1] School of Electronics Engineering,Universidad Santo Tomás, Tunja 150002, Colombia
[2] Department of Electronics Engineering, Pontificia Universidad Javeriana, Bogotá 110311, Colombia; manuel.perez@javeriana.edu.co (M.P.); diego-mendez@javeriana.edu.co (D.M.)
* Correspondence: william.chaparro@usantoto.edu.co
† These authors contributed equally to this work.

Abstract: Analyzing the conditions of use and selecting which technology is more efficient to apply is required when transmitting information through wireless networks.The Internet of Things (IoT) has gained traction in industry and academia as a paradigm in which information and communication technologies merge to deliver unique solutions by detecting, actuating, calculating, and sharing massive volumes of data via embedded systems. In this scenario, Low-Power Wide-Area Networks (LPWAN) appear to be an attractive solution for node connectivity. Typical IoT solutions demand flexible restrictions for wireless communication networks in terms of data rates and latency in exchange for having larger communication ranges and low energy consumption. Nonetheless, as the amount of data and data speeds demanded for particular applications increase, such as image transmissions, IoT network connectivity deteriorates. This paper proposes a communication architecture for image transmission across LPWAN networks utilizing LoRa modulation. The framework combines image processing techniques (classification, compressive sensing (CS), and reconstruction) with an investigation of LoRa modulation parameters using a Software-Defined Radio (SDR) environment. The results show that is possible to communicate an image of 128 × 128 pixels with four packets and one frequency channel in 2.51 s.

Keywords: Internet of Things (IoT); low-power wide-area networks (LPWAN); LoRa; compressive sensing; software-defined radio (SDR); image transmission

Citation: Chaparro B., F.; Pérez, M.; Mendez, D. A Communication Framework for Image Transmission through LPWAN Technology. *Electronics* **2022**, *11*, 1764. https://doi.org/10.3390/electronics11111764

Academic Editor: Sotirios K. Goudos

Received: 25 April 2022
Accepted: 26 May 2022
Published: 2 June 2022

1. Introduction

Communication and information technologies are becoming increasingly vital in our daily lives. Smart cities, agricultural monitoring, sensors service control, telemetry, smart grids, smart homes, smart health services, and human-body signal monitoring are just a few of the applications that have emerged since the advent of the Internet of Things (IoT) concept. Because the nature of the sensed data includes simple environmental variables, most IoT applications rely on the transmission of a small amount of data over a long distance. However, when data information increases in long-distance transmissions, IoT communication networks are limited, especially when looking for cost-effective and scalable solutions. Because of their high operational costs and limited coverage, particularly in remote areas, cellular networks are rarely used for agricultural applications. Unlicensed Low-Power Wide-Area Network (LPWAN) technologies have gained popularity due to their appealing characteristics, which include long range, scalability, low operational cost, and low energy consumption. Nonetheless, due to their limited capacity, unlicensed LPWAN-based solutions are still limited when it comes to transporting a large amount of data [1–11].

As previously stated, LPWAN technologies can be classified based on the frequency bands in which they operate: licensed bands such as LTE-M, Extended coverage 2G, and

NB-IoT. Additionally, they operate in unlicensed bands such as l SigFox, On-Ramp, and LoRaWAN. In terms of design goals, both types of LPWAN networks have advantages and disadvantages [12,13].

LoRaWAN was used in this work, and its modulation in particular was investigated due to its flexibility in terms of adaptive data rate and noise robustness. LoRaWAN is one of the most prominent LPWAN technologies, with a network deployed in over 77 countries and over a billion end-device connections. LoRaWAN operates at 868 MHz in Europe and 915 MHz in North America in the sub-GHz Industrial, Scientific, and Medical (ISM) frequency bands [12]. The LoRaWAN modulation scheme, also known as LoRa, employs a spread spectrum technique with a payload of 222 bytes per message [7,10,11]. Under these conditions, the number of messages to send for an IoT application where regular images must be transmitted is prohibitively large, and the transmission time is a couple of hours given the spectrum access restrictions of ISM bands. For example, in the best scenario with 500 kHz of bandwidth (BW) and a Spreading Factor (SF) of 7, the time over the air (ToA) for transmitting an image larger than 15 kbytes is around 100 ms per message. Furthermore, taking into account the ISM frequency band policies, which require a duty cycle of 1% for every single transmission (ETSI EN 300 220-1) [14], the total time exceeds 5 h, which is prohibitively long for any IoT application. With the same SF and BW conditions, but frequency hopping between 915 and 928 MHz (implemented between channels with no contiguity [14]), the time is around 3 min, not including saturation, collisions, and other problems associated with the use of shared spectrum. Image transmission is a challenging issue in both cases, and it is a general problem addressed in the literature for LPWAN networks, particularly when high data rates with low power consumption and long communication range are required [15–18].

As a result, a framework for transporting images using LoRa modulation without affecting features such as duty cycling, frequency hopping, or the use of multiple nodes to transmit different information packets simultaneously has been developed [13,19–23]. The communication system was developed on Software-Defined Radios (SDR) for LoRa information packet transmission and reception in order to have complete control over the LoRa modulation features. Because the SDR approach allows for more degrees of freedom than LoRa commercial radios, characteristics such as bandwidth, transmission power, spreading factor, preamble sequence definition, and sync sequence chirps definition can be easily adapted (even beyond the standard values) to meet the needs of the application. The implementation features of the framework are described in this paper, which include image processing, image classification, compressing sensing, postprocessing, and image reconstruction techniques. The structure of the papers is as follows: In Section 2, previous work is given. Section 3 describes the proposed framework. Section 4 presents the analysis results. In Section 5 the discussion is presented. Finally, Section 6 presents the conclusions.

2. Related Work

Many works have presented LPWAN design goals, requirements, and features [24–28]. All of them concluded LPWANs are the most suitable network solution for massive IoT system deployments over large areas with energy-efficient working schemes, low-cost and low-complexity end-devices, low data rates, and high latency. With a wide variety of LPWAN technologies, there has been a growing interest in the evaluation and comparison of the network performances, in particular the ones working in unlicensed frequency bands. LoRaWAN is one of the most representative LPWAN technologies which operate in sub-GHz Industrial, Scientific, and Medical (ISM) frequency bands at 868 MHz in Europe and 915 MHz in North America. This technology has been widely deployed in more than 77 countries worldwide, reaching billions of end-device connections [29]. LoRAWAN is a proprietary technology based on LoRa physical (PHY) layer which brings large coverage, low energy consumption, and low data rates. LoRaWAN was developed in North America by Semtech, IBM, Actility, and Microchip. The LoRaWAN network is single-hop where end-devices or motes are connected directly to a LoRAWAN base station acting as the gateway

to the information server. LoRa PHY is based on a Chip Spread Spectrum (CSS) modulation. CSS is a subcategory of direct-sequence spread spectrum (DSSS) that takes advantage of the controlled frequency diversity to recover data from weak signals, even near the noise level. CSS modulation was used in military communications due to the relatively low transmission power requirements, robustness to channel degradation, multipath, fading, Doppler effect, and jamming interference [30].

Recently, a growing interest in LPWAN technologies has appeared and several works have reported different contributions in the comparison, evaluation, and application of LPWAN. In this regard, LoRaWAN has taken particular relevance due to its flexible and configurable characteristics, for instance, in the work of [31,32], a realistic testbed for LoRaWAN network is presented; other works have explored energy consumption schemes for LoRAWAN networks [33–36], the extension of network coverage in urban areas [37,38], improvements for the Adaptative Data Rate (ADR) of LoRa modulation technique [39–41], and wireless systems solutions combined with the use of 5G systems [42,43]. Among the different LoRaWAN network implementations, platforms such as DPP2-CC430, DPP-SX1262, and SX1276 are mainly used [5,31,37,44–48]. Other works have produced analytic and simulation cases, where LoRaWAN network performance features such as Bit Error Rate (BER) and Signal-to-Noise Ratio (SNR) are obtained [49,50]. In addition, there has been an increasing interest to investigate optimal modulation parameters in LoRaWAN, such as the Spreading Factor (SF), modulation bandwidth, and transmission power for improving data rate, collision avoidance, resource allocation, and latency. In this regard, multiple techniques and evaluation scenarios have been recently proposed, some of them include fair ADR algorithms [51], time-slotted spreading factor hopping schemes for mitigating blind spots [52], performance evaluation in building environments [53], collision avoidance resource allocation techniques [54], experimental evaluation of LoRa packet reception [55], radio channel evaluation of massive node deployment [56], traffic evaluation studies [57], enhanced data transmission techniques [58], integration with cognitive radio schemes [59], secure firmware updates with adaptive data rate techniques [60], and the study of the wireless propagation of LoRa chirp radio signals over the water of rivers in tropical regions [61].

From the application point of view, LoRaWAN has encountered a relevant place as the network solution for IoT services. Thus, in [62] a LoRa sensor network for monitoring pastured livestock location is presented. In [63], an air quality monitoring and improvement system based on wireless sensor and actuator networks using LoRa communication is proposed. In [64], a development for air quality monitoring and gas leakage events with the LoRa sensor network is presented. The work in [65] presents several low-cost solutions using novel user interfaces and wireless communication technologies for monitoring irrigation systems. In [66], a new LoRa-like receiver is proposed to improve the robustness of symbol decoding to synchronization errors for satellite communications. In [67], a rural healthcare IoT architecture with the use of LoRa is shown. In [68], the development of a smart irrigation system is presented with enhanced coverage in urban areas thanks to the use of LPWAN sensor nodes based on LoRa and LoRaWAN. In [69], a farm monitoring system which incorporates unmanned aerial vehicles (UAVs), and LoRa technology for farm management and operation is presented. In [70], a smart campus proposal is presented with the use of LoRa. Ref. [71] presents the results of a study promoted by the Lisbon city council for trialing LPWAN technology for waste management. The work in [72] presents a traffic flow detection system based on LoRa, mainly focused on traffic conditions monitoring for accidental risk reduction in highways.

Image transmission on LoRaWAN has already been tackled by many authors in the literature. In [15], a monitoring method with image sensors communicating over the LoRa physical layer was presented. The authors proposed a scheme for overcoming the bandwidth limitation on LoRa. The transmitter and receiver node consists of a LoRa Arduino shield that comprises an RN2903 transceiver stacked on an Arduino Mega microprocessor. The experimental setup is composed of an Adafruit TTL serial camera that captures a JPEG

image, then images are encrypted as hexadecimal data and split into packets to transfer via LoRa. Image postprocessing consists on the evaluation of the Peak Signal-to-Noise Ratio (PSNR) of the received image. Results use different SF values with different coverage ranges. Results with a typical SF value of 7 show a total transmission packets of 314 with a transmission time of 67 s. In addition, the number of transmitted images were 21, where only 12 were successfully received. Some important features such as image size, medium-access duty cycle, shipping time, and LoRa symbol forms are not presented. The work in [73] presents a low-cost, low-power, long-range image sensor. The proposed system uses a Teensy 3.2 board as the host microcontroller to drive the CMOS uCamII camera capable of providing JPEG bitstream. First, the authors retrieve raw 128 $\times$ 128 (8 bits per pixel) greyscale images, then image compression on the board is carried out on the embedded system. The authors use an encoding scheme proposed in [74] where image compression is carried out by independent coding blocks to ensure that data packets are decodable and correctly received at the sink, and the de-correlation of neighboring blocks must be performed before packet transmission by appropriate interleaving methods to ensure that error concealment algorithms can be efficiently processed on the received data.

The proposal presented in [74] uses a discrete cosine transformation for image compression. The result of this compression scheme is a JPEG-like coder and operates on 8 $\times$ 8 pixel blocks with advanced optimizations on data computation to keep the computational overhead low. In addition, an optimized pixel interleaving scheme based on Torus Automorphisms is used [75]. Data are transmitted in different packets, with an interleaving scheme for retrieving enough information to obtain an approximation of the original value without affecting the energy consumption and time of use, or complexity of the image reconstruction process. The reconstructed image quality is acceptable until 80%. The LoRa module in Air9 from Modtronix with the reference SX1276 chip is used in the implementation. In the transmission test, an image can be completely sent with a number of information packets between 8 and 10. The system operates in a range of 1800 m without packet loss. This results are obtained when at least 50% of the original information is needed in order to recover the image without considerable losses. The work in [18] presents a medium-access mechanism to implement an image sensor with LoRa technology. An adapted Carrier Sense Multiple Access (CSMA) mechanism is presented for avoiding packet collision and packet losses. The mechanism is combined with a shared active time frame schedule technique to mitigate duty cycle issues. Thus, a high trade-off between image size and visual quality is presented. This feature gives the possibility to transport an image size between 900 to 1200 bytes, which can be encapsulated into five LoRa packets. The work in [16] proposes a low-power wide-area network protocol, which combines the LoRa modulation technique with embedded microprocessor technology. The proposal network is composed of three LoRaWAN nodes that provide three physical channels. The camera node allows bidirectional communications where each uplink transmission is followed by two short downlink windows. When the camera node needs to upload the data, it randomly selects a channel to execute channel activity detection. The proposal only gives a theoretical analysis without real testbed implementation. The work in [76] presents a method to transmit continuous images through LoRa. The samples are taken from a camera in a static environment where the critical challenge is to reduce the amount of transmitted data while preserving the image quality. The image-splitting technique consists on the use of grid patches that are only transmitted when there is an image modification based on a dissimilarity measure. The implementation and evaluation were on Raspberry Pi for data compression and an Arduino Uno with LoRa shield for data transmission.

The work in [77] aims to review the available methods applied to transfer images via LoRa infrastructure. The limitations of each method are pointed out, and the challenges that need to be managed in the future are also defined toward establishing a reliable image transfer over a LoRa network. A review of the LoRa approaches toward transmitting visual data was presented. Only few methods explore the modification of the LoRa physical layer to overcome the packet collision problem, and few methods deal with the compact image

representation. Table 1 presents a summary of the methods found in the literature for image transmission through LoRaWAN, where parameters such as transmission time, number of packets, and the employed image compression method are presented.

Table 1. Image transmission through LoRaWAN networks.

Reference	Method	Transmission Time (One Image) (Min)	Packets Number	Image Compression Method
Pham, 2016 [73]	Image compression Discrete Cosine Transform	-	8–10	JPEG
Kirichek et al., 2017 [78]	Fragmentation data	6	700	JPEG/JPEG2000
Jebril et al., 2018 [15]	Data encrypted hexadecimal	1.1	314	JPEG
Pham, 2018 [18]	CSMA (avoid collisions)	-	5	JPEG
Fan and Ding, 2018 [16]	Multiple out single in	-	-	-
Chen et al., 2019 [79]	MPLR protocol Tx/Rx	0.3	-	-
Ji et al., 2019 [76]	Image processing (Only transmits data with change)	-	-	-
Wei et al., 2020 [80]		1	85	JPEG
Juliando et al., 2021 [81]	-	858	-	-

3. Proposed Framework

The proposed framework (Figure 1) is designed in four stages. In stage I, image processing and classification techniques are implemented. In stage II, compression techniques are used in order to reduce the image information, and thus facilitate data transmission through LoRa. Stage III includes image transmission implemented on SDR platforms. Finally, in stage IV, postprocessing and reconstruction techniques are implemented.

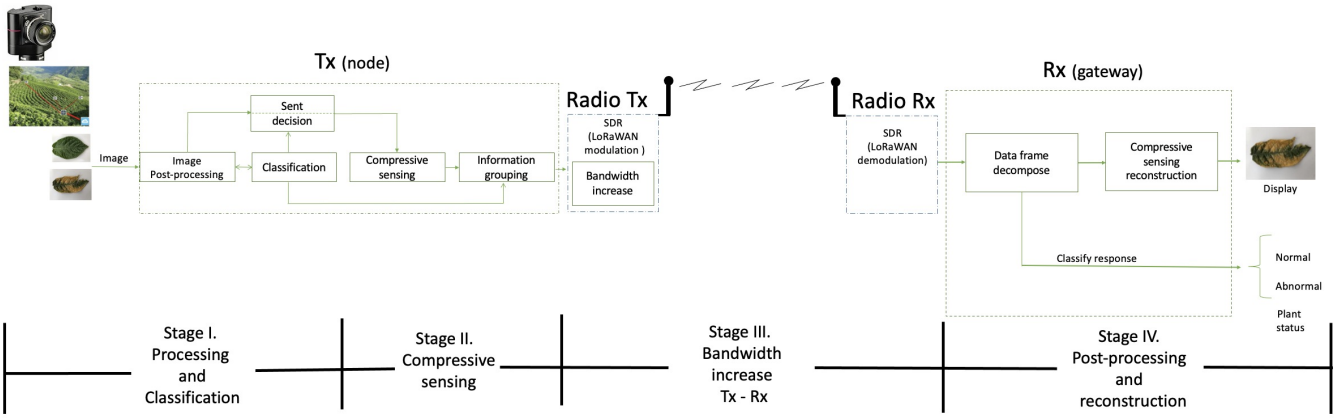

Figure 1. Framework to transmit and receive LoRa symbols.

3.1. Stage I: Processing and Classification

In the transmitter node, image processing was used to classify images and reduce the amount of data in an image using compressive sensing. The image data is transformed using a wavelet representation base [74,82–88]. As a result, this transformation unites the samples and reduces the variability of the original data. In this work, wavelet transforms prior to evaluation is used in between Kronecker, Discrete Cosine, and wavelet transforms. Furthermore, this process reduces data dispersion and allows for greater efficiency in the compression process. Similarly, the receiver used the inverse wavelet transformation to recover the original data.

3.2. Stage II: Compressive Sensing

A picture is a rectangular array of dots with m rows and n columns. The expression $m \times n$ is known as image resolution, and the dots are commonly referred to as pixels. The term resolution is also used to describe the number of pixels in an image per unit length. A monochromatic image (also known as a bilevel image) has pixels with one of two values, 0 or 1, that correspond to black or white colors and is considered the simplest type of image. A pixel in a grayscale image can have one of the n values be 0 through $n-1$, indicating one of 2^n, where n can be $4, 8, 12, 16, \ldots$. A continuous-tone image can have many similar colors (or grayscales) that are difficult for the eye to distinguish. A discrete-tone image is typically an artificial image with a few or many colors that lacks the noise and blurring of a natural image. A cartoon image has a color image made up of uniform areas, with each area having a uniform color but adjacent areas having very different colors. Each type of image clearly has feature redundancy, but they are redundant in different ways. As a result, any given compression method may not work well for all images, and different methods are required to compress the various image types [86].

Because modern hardware can display many colors, a pixel is commonly represented as a 24-bit number (R–G–B components, each of which occupies 8 bits). As a result, a 24-bit pixel can specify 1 to 2^{24} million colors, so an image with a resolution of 128 $\times$ 128 pixels occupies 49,152 bytes (16,384 in each component), one with 512 $\times$ 512 pixels occupies 786,432 bytes, and one with 1024 $\times$ 1024 pixels occupies 3,145,728 bytes. Then, image compression is critical. In general, information can be compressed if it is redundant; however, there is a concept known as "remove irrelevancy", which allows an image to be compressed with loss by removing irrelevant information even if the image contains no redundancy [86]. The spatial redundancy principle is used in image compression; as a result, if we select a random pixel in an image, its neighbors may have the same or similar colors, implying that the neighboring pixels are highly correlated. It is possible to rebuild the original data with high efficiency using this information.

Compressive Sensing (CS) can reduce information by up to 95% of its original size. Only 5% of the original vector information can be rebuilt with high precision. This allows for a reduction in the amount of data that must be transported into LoRa. CS is a technique for creating and retrieving sparse signals with low noise using far fewer samples than the Nyquist sampling theorem requires [89,90]. To implement CS, a program that represents the original signal in a sparse signal using an appropriate sparse representation was used. The original signal can be represented as a $N \times 1$ vector, where N is equal to $N = n \times n \ \ [rows] \times [columns]$.

CS employs a sparsity technique to transform an information signal denoted as s into a vector $S \ \in \ R^N$ in discrete form. k (data value dispersion relation) and s are elements of the original signal that differ from zero (the most representative). Signals with low dispersion (high value of k) can be converted to signals with greater dispersion via lineal transformation f by $f = s$ and $f \in R^{N \times N}$, which in our case represents data on wavelet transform [82,91–95].

A k-disperse signal in which $f \in R^N$ are sampled with CS to produce the $g \in R^M$ signal, where $M << N$. A system sampling matrix is a representation of the sampling in matrix form as $g = f$ and $\in R^{M \times N}$. If f is unknown, an indeterminate system of linear equations can be found (infinite solutions). It could be solved for this purpose with an optimization problem that can be converted into a complex mathematical problem that is not convex. Another approach is to use a sensing matrix with algorithms such as Iterative Hard Thresholding (IHT), Orthogonal Matching Pursuit (OMP), Gradient Projection for Sparse Reconstruction (GPSR), or Two-Step Iterative Shrinkage/Thresholding (Twist) [90,96–98]. Previous research evaluated these algorithms, and the results enable us to select Twist as the best output in our case. We can reduce the computational process, data payload, processing time, and energy consumption with the help of CS.

3.3. Stage III: Transmission Bandwidth Increase

Initially, our research looked into the possibility of discovering a method to increase bandwidth. Techniques such as diversity, Multiple In Multiple Out (MIMO), Single In Multiple Out (SIMO), and others were investigated; however, the results indicate that for our framework they are not required. As a result, we focus on implementing LoRa modulation in Software-Defined Radios (SDR) in the transmitter and receiver, allowing us to have more degrees of freedom than LoRa commercial radios in terms of bandwidth, transmission power, spreading factor, preamble sequence definition, and sync sequence chirps definition. LoRa features can be optimized to achieve higher data rates by taking advantage of the flexibility provided by SDR. Test results show that high bandwidth (>500 kHz) results in higher capacity and lower SF values (SF7), resulting in data rates around 50 kbps with good sensitivity at reception, even near noise floor values. This result is adjusted by having a large payload, a short overhead, and using low coding rates [48,99–106].

3.4. Stage IV: Postprocessing and Reconstruction

The data sent by the radio transmitter is received by the reception node at this stage. These data are processed through data frame decomposition in order to organize and deliver classification information, as well as image reconstruction. The classification result and reconstructed images are displayed by the reception node. The received data is processed, and once rebuilt, the vector with its features is used in a sparse representation reconstruction algorithm to recover a large number of samples of the original signal and recover the original information vector via wavelet inverse transform. It is now necessary to change the matrix's original size from $M \times N$ to $n \times n$ and display the image. To compare the original image with the received image, the PSNR function was used, which can be calculated as (1).

$$PSNR = 10log\left(\frac{S^2}{MSE}\right) \tag{1}$$

where s is 255 in an image of 8 bits and MSE is the mean squared error, which is the average of the squared difference in the intensity pixels in the original and the output images. MSE is calculated with (2).

$$MSE = \frac{1}{mn}\sum_{i=0}^{m-1}\sum_{j=1}^{n-1}[I(i,j) - K(i,j)]^2 \tag{2}$$

where m and n are the respective length and width of the image in pixels, and $I(i,j)$ and $K(i,j)$ are functions that describe the intensity of individual pixels in the transmitted and received image. PSNR allows calculating the relation between transmitted and received images. It is expressed in a logarithmic scale where values of among 30 and 50 dB are acceptable [87,95]. In wireless communication systems, acceptable values are considered from 20 to 25 dB [107,108]. If the image on analysis is the same as the reference, the PSNR is infinite [86].

3.5. Framework Interconnection

3.5.1. LoRa PHY Modulation

LoRa PHY is based on a Chip Spread Spectrum (CSS) modulation. CSS is a subcategory of DSSS that takes advantage of the controlled frequency diversity to recover data from weak signals, even near the noise level. In CSS, the SF is the number of transmitted bits in a symbol by considering the number of symbols in chips of 2^{SF}. The SF is defined in (3), which is related with spread bandwidth BW, the symbol rate R_s, and the chirp duration $T = \frac{1}{R_s}$ through Equation (4).

$$SF = \frac{chip\ rate}{symbol\ rate} \tag{3}$$

$$2^{SF} = \frac{BW}{R_s} = BW\,T \tag{4}$$

The basic element of LoRa–CSS modulation is the chirp, and its waveform is written in (5).

$$S_{css}(t) = \begin{cases} e^{j\phi(t)}, & \text{if } -\frac{T}{2} \leq t \leq \frac{T}{2} \\ 0, & otherwise \end{cases} \tag{5}$$

where, $\phi(t)$ is a chirp phase. From [13,50], by taking the relationship of the instantaneous frequency with the phase $f(t) = \frac{1}{2\pi}\frac{d\phi(t)}{dt}$ and combining with the definition in (4), the LoRa raw chirp signal of (5), in one chirp duration T it is reduced to (6).

$$S_{css}(t) = e^{j\left(2\pi\ \frac{BW}{T}\ \frac{t^2}{2}\right)} \tag{6}$$

The chirp may code up to $SF = 12$ bits during a chirp period by shifting the frequency increasing ramp based on the 2^{SF} possible chip values. Thus, each chip code is obtained by a cyclic shift of the chirp reference. A coded chirp signal is expressed in (7), where k is the number of shifted chips [13].

$$S_{css}(t) = e^{j\left(2\pi\ \frac{BW}{T}\ \frac{(t-k/BW)^2}{2}\right)} \tag{7}$$

At the receiver, the signal is processed through a matched filter technique by correlating a known raw down-chirp signal with the unknown coded up-chirp signal in order to detect the presence of the shift. In other words, the received coded up-chirp is convoluted with a conjugate time-reversed version of the raw signal. There are two time periods where a frequency shift of value BW occurs at the time index k, corresponding to the value of the coded symbol. Then, down-converting by sampling the signal at the chip rate BW, the instantaneous frequency becomes continuous over the whole chirp and, after subtracting the carrier, the instantaneous frequency is proportional to the shift k. The FFT of the sampled signal shows a flat response with a peak shifted by the coded symbol value.

3.5.2. Stage Flow Process

In stage I—processing and classification—the images are classified into normal or abnormal features. Thus, only the abnormal is transmitted between transmitter and receiver. Then, the abnormal samples are converted with wavelet transform. In stage II, the data is operated with CS, and its results give us a sparse vector with decimal and negative numbers. LoRa technology works with integer values among a range according to the spreading factor (SF) value. Thus, it was necessary to convert the sparse vector information into data supported in LoRa symbols. For this reason, it is necessary to encode the sparse vector. An encoder and decoder with an 8-bit structure were implemented. In stage III, it is necessary to create the LoRa symbols consequent with 8 bits, and therefore SF = 8 was implemented. Despite lower SF giving higher data rates for LoRa modulation, the SF's choice is to take into account the transmission of a compressed unit of the spare vector in one single LoRa chirp symbol, this simplifies the complexity of the reconstruction algorithm at the receiver at the expense of losing transmission data rates.

Then, using National Instruments NI-2920 cards, the transmission and reception of LoRa symbols were implemented on SDR. Modulation features such as SF, BW, and the sampling frequency in the transmitter were set in conjunction with the interpolation and decimation factor in the receiver in order to achieve the bandwidth to sweep the value set up in the transmitter. Some specific features, such as the operating center frequency, gain, number of samples, and decimation factor value, had to be adjusted at the receiver.

These values are required to operate within the operating frequency range. In our case, we needed to use a decimation factor that allowed us to sweep the BW used in the transmitter over 2 MHz of the spectrum around the central operation frequency (500 kHz). To restart the radio features, packet transmission and reception are required.

In stage IV, a sweep from the beginning of the received vector to the end was required. Preamble and synchronization chirp symbols are also considered at this stage, as they are required to locate the image's coded information. The received vector was then analyzed using the Fast Fourier Transform (FFT) to find a peak between the image's preamble and data chirp symbols. Signal peaks in the FFT signal transform allow us to determine the end of the preamble and the start of the synchronization symbols; after two synchronization symbols (two symbols times $2T$), we can determine the start of the data. Because the data were encoded in bytes, it was necessary to decode them in order to find the original values (wavelet transform representation). To accomplish this, a simple algorithm was developed that converts the received data back into its original form. Following the data decoding process, a vector of comparable length to the one transmitted is obtained. The resulting data contain information about the output wavelet transform values and positions, including negative values. Thus, the inverse wavelet transform is required, followed by taking the vector and adjusting the matrix with an original array, and finally representing the image and evaluating it with the PSNR function.

4. Analysis Results

The following results from the various stages of the proposal framework are presented. Thus, stage I demonstrated image processing in which the sparsity was evaluated using wavelet, Kronecker, and Discrete Cosine (DC) transforms. This seeks to establish a common foundation for improving information reduction. Figure 2 depicts the integration of stages I and II, where it is possible to observe the PSNR values versus sparsity percentage and conclude that when the sparcification percentage is increased, the wavelet transform achieves the best PSNR results. The coefficients of the DCT, wavelet, and Kronecker transforms are shown in Figure 3a–c. It is possible to see that wavelet has a minor data deviation, indicating an improvement in Stage II of compressive sensing.

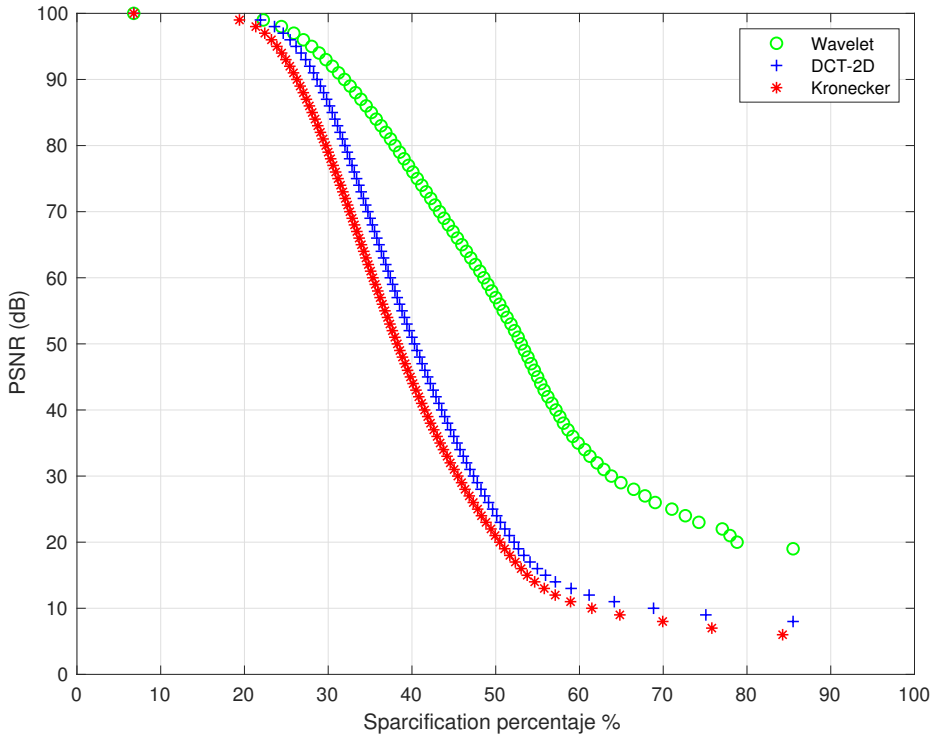

Figure 2. PSNR values vs sparcity percentage.

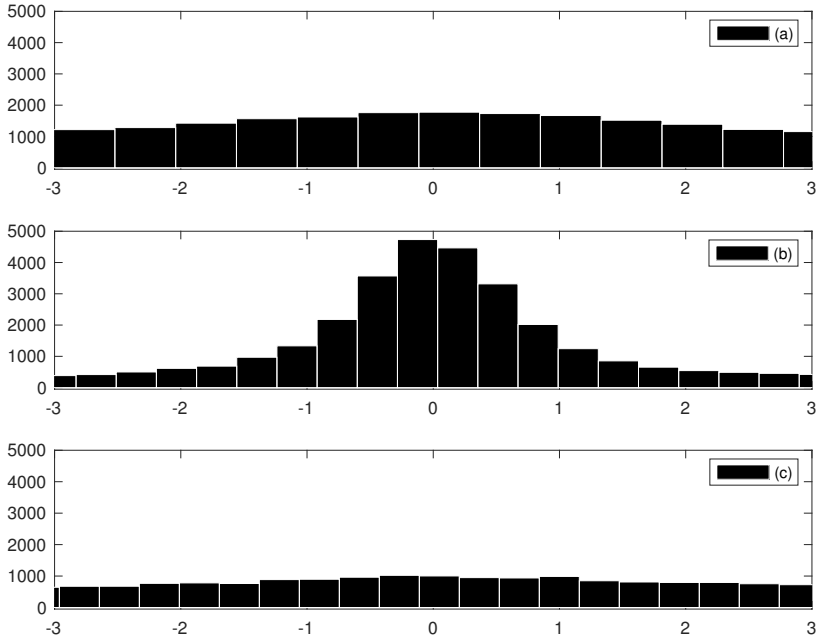

Figure 3. Coefficients distribution.

All algorithms (IHT, OMP, GPSR, and Twist) were used in the reconstruction process. The sparse vector signals and the sample matrix were used as inputs, and the outputs were a PSNR-based relationship between the rebuilt signal and the original signal, as well as the number of rebuilt samples (M). Figure 4 shows that the Twist algorithm achieves the highest reconstruction index in terms of M.

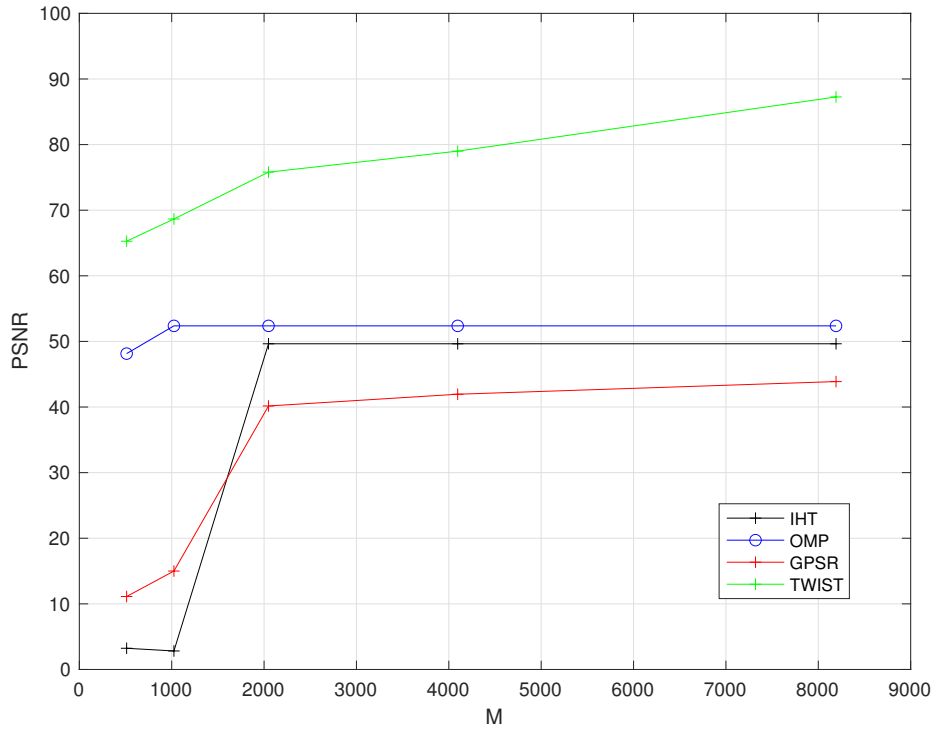

Figure 4. Reconstruction algorithms evaluation.

LoRa symbols were created using encoded data. As previously stated, preamble and synchronization chirp symbols are generated; in our case, 10 preamble symbols (up-chirps) and 2 synchronizations (down-chirps) were modulated before the start of the data

symbols to create the total LoRa frame to be transmitted on SDR platforms. It is important to remember that any chirp symbol (preamble, synchronization, or data) has the same symbol time, which is proportional to the value of SF. Figure 5 depicts LoRa symbols for an up-chirp, a down-chirp, and a data symbol created and transmitted on the SDR platform. Figure 6 illustrates the spectrogram of the transmitted LoRa frame signal, which contains symbols for 10 preamble up-chirps, 2 synchronization down-chirps, and coded data chirps.

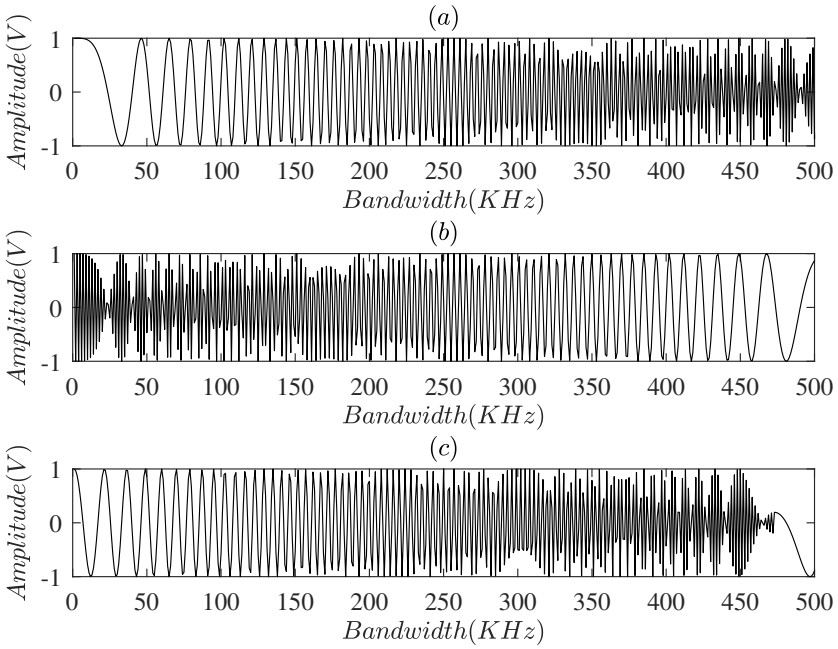

Figure 5. (**a**) up-chirp, (**b**) down-chirp, and (**c**) coded LoRa signal with $SF = 8$ and $BW = 500$ kHz.

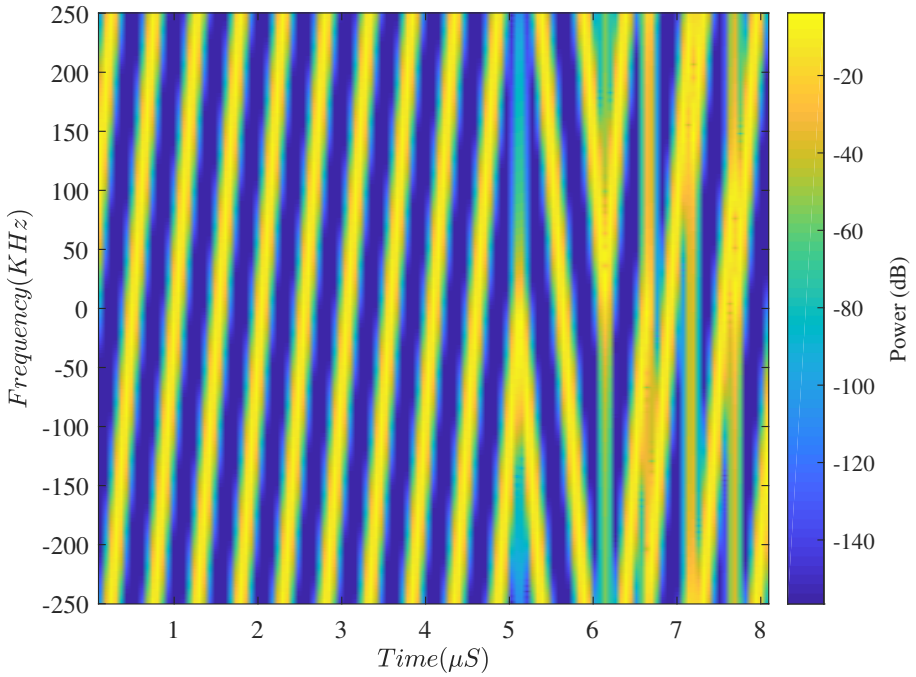

Figure 6. Transmission spectogram.

At the receiver of stage III, the operating frequency and the master click rate were configured on the SDR. The received chirps are presented in Figure 7 and the received spectrogram is presented in Figure 8. In stage IV, after the LoRa demodulation process, it is necessary to sweep from the beginning of the received vector until its end. Here, it

is considered the first symbols (10 of preamble and 2 of synchronization). These twelve symbols are necessary to retrieve the data in the received symbols. Figure 9 shows a complete received LoRa frame signal in time, where preamble synchronization and data are shown. Signal peaks allow to find the preamble and the synchronization chirp symbols, after two synchronization symbols ($2T$), it is possible to find the beginning of the data.

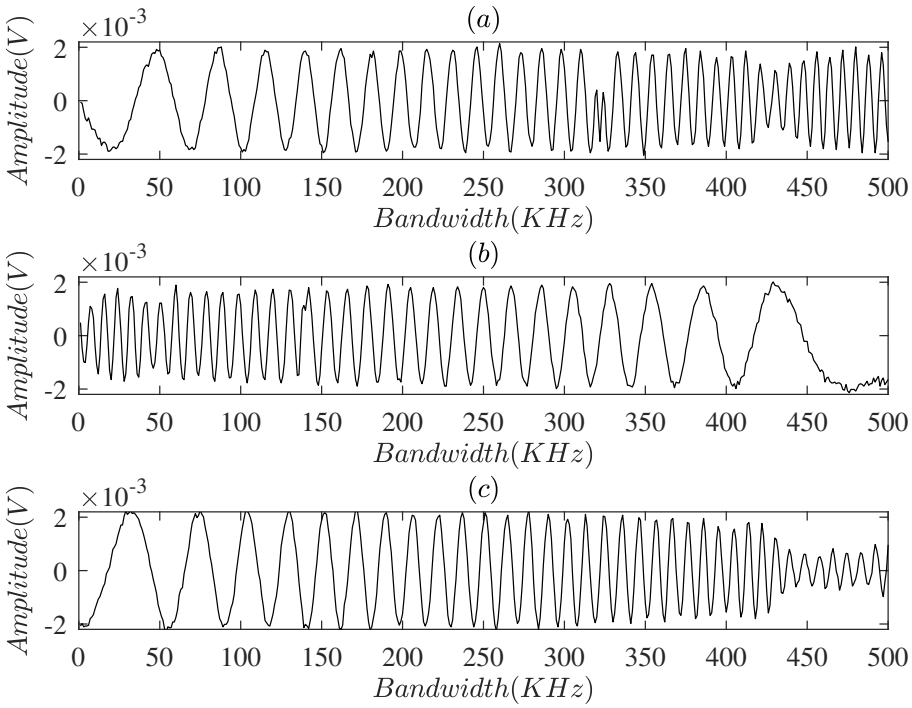

Figure 7. (**a**) up-chirp, (**b**) down-chirp, and (**c**) received coded LoRa signals.

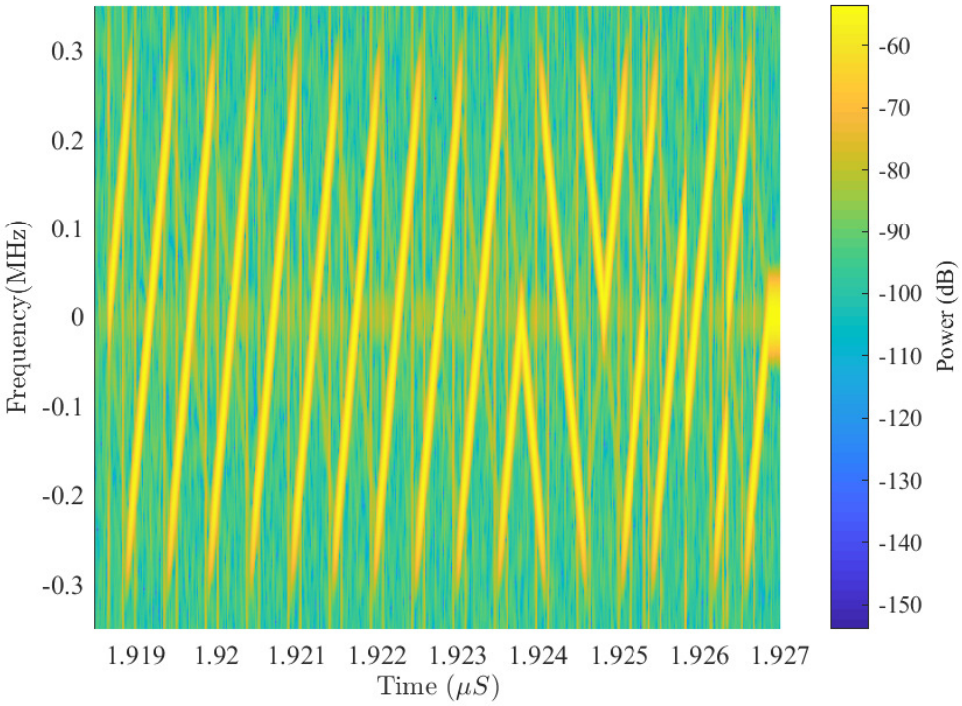

Figure 8. Reception spectrogram.

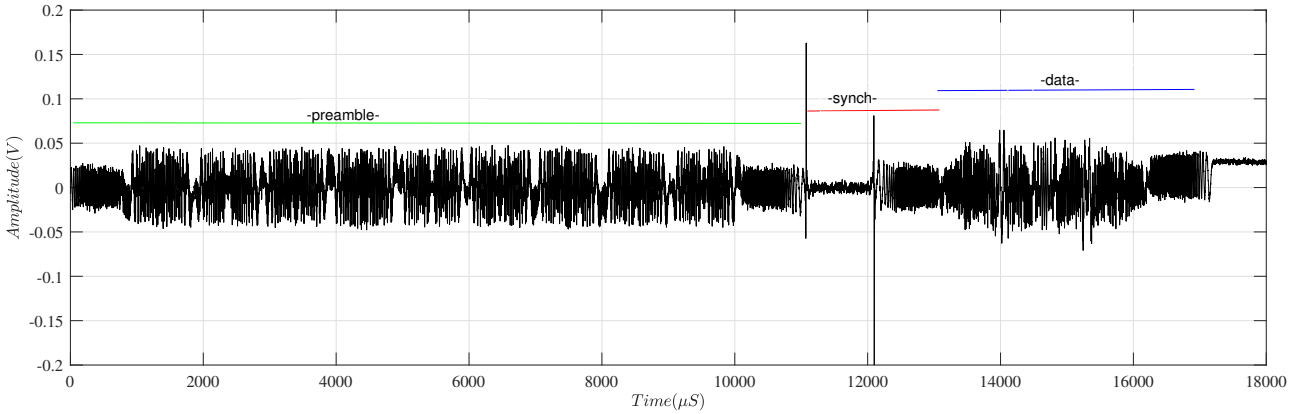

Figure 9. Real component of a received LoRa frame signal.

To decode the image information and find the original values (wavelet transform representation), a program was created that converts the received data (LoRa symbols) into their base representation again. Decoding the received data is required to restore the image. As a result, a vector of similar length must be integrated among the many packets received. This vector contains information on wavelet transform output values, positions, and negative value positions. After using the reconstruction procedure to rebuild the vector using their features, the original vector of information is recovered using wavelet inverse transform. Finally, the initial size of matrix nxn must be adjusted, and the image must be screened. The framework's final section illustrates the differences between the original and rebuilt images. Figure 10 depicts a sample of the original image in (a), a reconstructed image with a sparse percentage of 90 and a PSNR value of 30.02 dB in (b), and a sparse percentage of 95 and a PSNR value of 26.81 dB in (c).

(**a**) (**b**) (**c**)

Figure 10. (**a**) original image, (**b**) reconstructed image with a percentage of 90% sparsity with a PSNR of 30.02 dB, and (**c**) reconstructed image with a percentage of 95% sparsity with a PSNR of 26.81 dB.

5. Discussion

Wireless networks are used in a wide range of applications every day, LPWAN technologies are used in IoT scenarios, while their low data transfer capacity limits their use to low-payload applications. This article presents a framework to transport images through the use of LoRa modulation. Processing and classification, compressive sensing, transmission and receiving of LoRa symbols, postprocessing, and image reconstruction techniques were all employed for this goal.

Previous research has revealed how to transfer images using LoRaWAN networks. See Table 1. Nevertheless, there is very little information available about these proposals, and to

the best of our knowledge, there are no LoRa modulation implementations in transmitters and receivers with open platforms; thus, not only is a framework to transport images with a LoRa modulation into LPWAN networks shown, this work also shows how it can be implemented in SDR devices, allowing for future tests to improve the technology.

6. Conclusions

We have used this proposal to transport an image with LoRa modulation. Within our proposal, images of 128×128 pixels of information were taken. Thus, information can be reduced until 95% using processing and classification techniques and CS process. With only one frequency channel (ISM band) and four (4) packets, the transmission time for an image is decreased to 2.51 s. The usage of SDR devices in the implementation allows us to better understand this technology and work on possible protocol changes in the future.

Some remarks are presented to communicate images through LoRa modulation, thus is possible to observe:

1. Finding a way to capture the image directly in the crop is required because the image is placed on a neutral background in the manner given in this article. There are several conditions that must be met while taking a photograph in an uncontrolled environment, such as brightness, shades, angle of incidence of the sun, and more. These factors have an impact on the real image and can lead to representation and classification problems.
2. Integrate a complete system capable of taking an image, compressing it, transmitting and receiving, reconstructing the information, and finally displaying it. As a result, the phases must be integrated into the proposed framework, which executes the processes through an autonomous system that performs all of the processes independently.

Author Contributions: Conceptualization, F.C.B., M.P., D.M.; methodology, F.C.B., M.P., D.M.; software, F.C.B.; Validation, M.P., D.M.; formal analysis, F.C.B., M.P., D.M.; investigation , F.C.B.; resources, F.C.B., M.P., D.M.; data analysis, F.C.B., M.P., D.M.; writing and review, F.C.B., M.P., D.M.; visualization, F.C.B., M.P., D.M.; supervision, M.P., D.M. All authors have read and agreed to the published version of the manuscript.

Funding: This research is founded by Gobernación de Boyacá through the 733 and 922 Calls from the Science Ministry of Colombia (MinCiencias) 2015 and 2022, respectively. In addition, it is also founded by the Pontificia Universidad Javeriana and the Colombian Ministry of Information and Communication Technologies (MinTIC) through the project titled "Centro de Excelencia y Apropiación en Internet de las Cosas (CEA-IoT)" Grant ID: 7161, and the Universidad Santo Tomás.

Data Availability Statement: The datasets generated during this study are available on request from the corresponding author.

Acknowledgments: The authors would like to thank the Electronics Department and laboratory of the Pontificia Universidad Javeriana, for providing the required resources to conduct this study. Special thanks to professor Andrea Abrardo of the Universitá degli Studi di Siena in Italy, and Universidad Rey Juan Carlos in Spain for the given support.

Conflicts of Interest: The authors declare no conflict of interest.

Abbreviations

The following abbreviations are used in this manuscript:

IoT	Internet of Things
LPWAN	Low-Power Wide-Area Networks
CS	Compressive Sensing
LTE-M	Long-Term Evolution Machine
NB-IoT	Narrow Band-IoT
ISM	Industrial, Scientific, and Medical
SF	Spreading Factor
BW	Bandwidth
ToA	Time over the Air
SDR	Software-Defined Radio
PSNR	Peak Signal-to-Noise Ratio
CSMA	Carrier Sense Multiple Access
IHT	Iterative Hard Thresholding
OMP	Orthogonal Matching Pursuit
GPSR	Gradient Projection for Sparse Reconstruction
Twist	Two-Step Iterative Shrinkage/Thresholding
MIMO	Multiple In Multiple Out
SIMO	Single In Multiple Out
MSE	Mean Squared Error
FFT	Fast Fourier Transform

Appendix A

Math Symbols:

The math symbols are described in Appendix A.
The following math symbols are used in this article:
Compressing sensing:

- N: Information vector.
- n: Rows/columns of matrix.
- s: Signal.
- S: Vector.
- R: Image dimension.
- k: Dispersion relation.
- f: Linear transformation.
- M: Sampled information.

Postprocessing and reconstruction:

- S: Resolution vector.
- MSE: Mean Squared Error.
- m,n: Lenght nd width of image.
- I: Intensity of pixels in transmitter node.
- K: Intensity of pixels in receiver node.
- Scss: Chirp spread spectrum signal.
- t: Period.
- BW: Bandwidth.
- T_s: Symbol time.

References

1. Xiong, X.; Zheng, K.; Xu, R.; Xiang, W.; Chatzimisios, P. Low power wide area machine-to-machine networks: Key techniques and prototype. *IEEE Commun. Mag.* **2015**, *53*, 64–71. [CrossRef]
2. Petajajarvi, J.; Mikhaylov, K.; Hamalainen, M.; Iinatti, J. Evaluation of LoRa LPWAN technology for remote health and wellbeing monitoring. In Proceedings of the International Symposium on Medical Information and Communication Technology—ISMICT, Worcester, MA, USA, 20–23 March 2016; Volume 2016, pp. 1–5. [CrossRef]
3. Zanella, A.; Bui, N.; Castellani, A.; Vangelista, L.; Member, S.; Zorzi, M. Internet of Things for Smart Cities. *IEEE Internet Things J.* **2014**, *1*, 22–32. [CrossRef]

4. Kim, D.H.; Park, J.B.; Shin, J.H.; Kim, J.D. Design and implementation of object tracking system based on LoRa. In Proceedings of the 2017 International Conference on Information Networking (ICOIN), Da Nang, Vietnam, 11–13 January 2017; pp. 463–467. [CrossRef]
5. Augustin, A.; Yi, J.; Clausen, T.; Townsley, W. A Study of LoRa: Long Range & Low Power Networks for the Internet of Things. *Sensors* **2016**, *16*, 1466. [CrossRef]
6. Espinosa, M.; Perez, M.; Zona, T.; Lagrange, X. Radio Access Mechanism for Massive Internet of Things Services over White Spaces. *IEEE Access* **2021**, *9*, 120911–120923. [CrossRef]
7. Delgado-Ferro, F.; Navarro-Ortiz, J.; Chinchilla-Romero, N.; Ramos-Munoz, J.J. A LoRaWAN Architecture for Communications in Areas without Coverage: Design and Pilot Trials. *Electronics* **2022**, *11*, 804. [CrossRef]
8. Pathak, G.; Gutierrez, J.; Rehman, S.U. Security in low powered wide area networks: Opportunities for software defined network-supported solutions. *Electronics* **2020**, *9*, 1195. [CrossRef]
9. Marahatta, A.; Rajbhandari, Y.; Shrestha, A.; Singh, A.; Thapa, A.; Gonzalez-Longatt, F.; Korba, P.; Shin, S. Evaluation of a lora mesh network for smart metering in rural locations. *Electronics* **2021**, *10*, 751. [CrossRef]
10. Almuhaya, M.A.; Jabbar, W.A.; Sulaiman, N.; Abdulmalek, S. A Survey on LoRaWAN Technology: Recent Trends, Opportunities, Simulation Tools and Future Directions. *Electronics* **2022**, *11*, 164. [CrossRef]
11. Ugwuanyi, S.; Paul, G.; Irvine, J. Survey of iot for developing countries: Performance analysis of lorawan and cellular nb-iot networks. *Electronics* **2021**, *10*, 2224. [CrossRef]
12. Sanchez-Iborra, R.; Cano, M.D. State of the art in LP-WAN solutions for industrial IoT services. *Sensors* **2016**, *16*, 708. [CrossRef]
13. Goursaud, C.; Gorce, J.M. Dedicated networks for IoT: PHY/MAC state of the art and challenges. *EAI Endorsed Trans. Internet Things* **2015**, *1*, 150597. [CrossRef]
14. Agencia Nacional del Espectro-Colombia. Resolución ANE 0711 de 2016 Bandas ICM Colombia. Available online: http://www.ane.gov.co2016 (accessed on 25 April 2022).
15. Jebril, A.H.; Sali, A.; Ismail, A.; Rasid, M.F.A. Overcoming limitations of LoRa physical layer in image transmission. *Sensors* **2018**, *18*, 3257. [CrossRef] [PubMed]
16. Fan, C.; Ding, Q. A novel wireless visual sensor network protocol based on LoRa modulation. *Int. J. Distrib. Sens. Netw.* **2018**, *14*, 155014771876598. [CrossRef]
17. Georgiou, O.; Raza, U. Low Power Wide Area Network Analysis: Can LoRa Scale? *IEEE Wirel. Commun. Lett.* **2017**, *6*, 162–165. [CrossRef]
18. Pham, C. Enabling and deploying long-range IoT image sensors with LoRa technology. In Proceedings of the 2018 IEEE Middle East and North Africa Communications Conference—MENACOMM 2018, Jounieh, Lebanon, 18–20 April 2018; pp. 1–6. [CrossRef]
19. Blackstock, M.; Lea, R. IoT interoperability: A hub-based approach. In Proceedings of the 2014 International Conference on the Internet of Things—IOT 2014, Cambridge, MA, USA, 6–8 October 2014; pp. 79–84. [CrossRef]
20. Centenaro, M.; Vangelista, L.; Zanella, A.; Zorzi, M. Long-Range Communications in Unlicensed Bands: The Rising Stars in the IoT and Smart City Scenarios. *IEEE Wirel. Commun. Lett.* **2016**, *23*, 60–67. [CrossRef]
21. Chaves-Diéguez, D.; Pellitero-Rivero, A.; García-Coego, D.; González-Castao, F.J.; Rodríguez-Hernández, P.S.; Piñeiro-Gómez, Ó.; Gil-Castiñeira, F.; Costa-Montenegro, E. Providing iot services in smart cities through dynamic augmented reality markers. *Sensors* **2015**, *15*, 16083–16104. [CrossRef]
22. Margelis, G.; Piechocki, R.; Kaleshi, D.; Thomas, P. Low Throughput Networks for the IoT: Lessons Learned From Industrial Implementations. In Proceedings of the 2015 IEEE 2nd World Forum on Internet of Things (WF-IoT), Milan, Italy, 14–16 December 2015; Volume 1, pp. 181–186. [CrossRef]
23. Shahidul Islam, M.; Islam, M.T.; Almutairi, A.F.; Beng, G.K.; Misran, N.; Amin, N. Monitoring of the Human Body Signal through the Internet of Things (IoT) Based LoRa Wireless Network System. *Appl. Sci.* **2019**, *9*, 1884. [CrossRef]
24. Shanmuga Sundaram, J.P.; Du, W.; Zhao, Z. A Survey on LoRa Networking: Research Problems, Current Solutions, and Open Issues. *IEEE Commun. Surv. Tutor.* **2020**, *22*, 371–388. [CrossRef]
25. Chen, Y.; Sambo, Y.A.; Onireti, O.; Imran, M.A. A Survey on LPWAN-5G Integration: Main Challenges and Potential Solutions. *IEEE Access* **2022**, *10*, 32132–32149. [CrossRef]
26. Ayoub, W.; Samhat, A.E.; Nouvel, F.; Mroue, M.; Prévotet, J.C. Internet of Mobile Things: Overview of LoRaWAN, DASH7, and NB-IoT in LPWANs Standards and Supported Mobility. *IEEE Commun. Surv. Tutor.* **2019**, *21*, 1561–1581. [CrossRef]
27. Chaudhari, B.S.; Zennaro, M.; Borkar, S. LPWAN Technologies: Emerging Application Characteristics, Requirements, and Design Considerations. *Future Internet* **2020**, *12*, 46. [CrossRef]
28. Buurman, B.; Kamruzzaman, J.; Karmakar, G.; Islam, S. Low-Power Wide-Area Networks: Design Goals, Architecture, Suitability to Use Cases and Research Challenges. *IEEE Access* **2020**, *8*, 17179–17220. [CrossRef]
29. LoRaWAN Coverage Map. Available online: https://lora-alliance.org (accessed on 18 November 2021).
30. Stan, V.A.; Timnea, R.S.; Gheorghiu, R.A. Overview of high reliable radio data infrastructures for public automation applications. In Proceedings of the ECAI 2016—International Conference—8th Edition Electronics, Computers and Artificial Intelligence, Ploiesti, Romania, 30 June–2 July 2016; pp. 978–981. [CrossRef]

31. Trüb, R.; Forno, R.D.; Gsell, T.; Beutel, J.; Thiele, L. A testbed for long-range LoRa communication. In Proceedings of the 2019 18th ACM/IEEE International Conference on Information Processing in Sensor Networks (IPSN), Montreal, QC, Canada, 16–18 April 2019; pp. 342–343. [CrossRef]
32. Kim, S.; Lee, H.; Jeon, S. An adaptive spreading factor selection scheme for a single channel lora modem. *Sensors* **2020**, *20*, 1008. [CrossRef] [PubMed]
33. Singh, R.K.; Puluckul, P.P.; Berkvens, R.; Weyn, M. Energy consumption analysis of LPWAN technologies and lifetime estimation for IoT application. *Sensors* **2020**, *20*, 4794. [CrossRef]
34. Dos Anjos, J.C.; Gross, J.L.; Matteussi, K.J.; González, G.V.; Leithardt, V.R.; Geyer, C.F. An algorithm to minimize energy consumption and elapsed time for iot workloads in a hybrid architecture. *Sensors* **2021**, *21*, 2914. [CrossRef]
35. Maudet, S.; Andrieux, G.; Chevillon, R.; Diouris, J.F. Refined node energy consumption modeling in a LoRaWAN network. *Sensors* **2021**, *21*, 6398. [CrossRef]
36. Ould, S.; Bennett, N.S. Energy Performance Analysis and Modelling of LoRa Prototyping Boards. *Sensors* **2021**, *21*, 7992. [CrossRef]
37. Sagir, S.; Kaya, I.; Sisman, C.; Baltaci, Y.; Unal, S. Evaluation of Low-Power Long Distance Radio Communication in Urban Areas: LoRa and Impact of Spreading Factor. In Proceedings of the 2019 7th International Conference on Digital Information Processing and Communications—ICDIPC 2019, Trabzon, Turkey, 2–4 May 2019; pp. 68–71. [CrossRef]
38. Liao, C.H.; Zhu, G.; Kuwabara, D.; Suzuki, M.; Morikawa, H. Multi-Hop LoRa Networks Enabled by Concurrent Transmission. *IEEE Access* **2017**, *5*, 21430–21446. [CrossRef]
39. Hauser, V.; Hegr, T. Proposal of Adaptative Data Rate Algorithm for LoRaWAN-based Infraestructure. In Proceedings of the IEEE 5th International Conference on Future Internet of Things and Cloud, Prague, Czech Republic, 21–23 August 2017; pp. 1–6. [CrossRef]
40. Marais, J.M.; Member, S.; Malekian, R.; Member, S.; Low-power, A. Evaluating the LoRaWAN Protocol Using a Permanent Outdoor Testbed. *IEEE Sens. J.* **2019**, *19*, 4726–4733. [CrossRef]
41. Kufakunesu, R.; Hancke, G.P.; Abu-Mahfouz, A.M. A survey on adaptive data rate optimization in lorawan: Recent solutions and major challenges. *Sensors* **2020**, *20*, 5044. [CrossRef]
42. Hsiao, S.J. Employing a Wireless Sensing Network for AIoT Based on a 5G Approach. *Electronics* **2022**, *11*, 827. [CrossRef]
43. Kansal, L.; Berra, S.; Mounir, M.; Miglani, R.; Dinis, R.; Rabie, K. Performance Analysis of Massive MIMO-OFDM System Incorporated with Various Transforms for Image Communication in 5G Systems. *Electronics* **2022**, *11*, 621. [CrossRef]
44. Petrić, T.; Goessens, M.; Nuaymi, L.; Toutain, L.; Pelov, A. Measurements, Performance and Analysis of LoRa FABIAN, a real-world implementation of LPWAN. In Proceedings of the Personal, Indoor, and Mobile Radio Communications (PIMRC), Valencia, Spain, 4–7 September 2016; pp. 104–110. [CrossRef]
45. Bharadwaj, A.S.; Rego, R.; Chowdhury, A. IoT based solid waste management system: A conceptual approach with an architectural solution as a smart city application. In Proceedings of the 2016 IEEE Annual India Conference (INDICON), Bangalore, India, 16–18 December 2016; pp. 1–6. [CrossRef]
46. Bor, M.; Vidler, J.; Roedig, U. LoRa for the Internet of Things. In Proceedings of the 2016 International Conference on Embedded Wireless Systems and Networks, Graz, Austria, 15–17 February 2016; pp. 361–366.
47. Haghighi, M.; Qin, Z.; Carboni, D.; Adeel, U.; Shi, F.; McCann, J.A. Game theoretic and auction-based algorithms towards opportunistic communications in LPWA LoRa networks. In Proceedings of the 2016 IEEE 3rd World Forum on Internet of Things, WF-IoT 2016, Reston, VA, USA, 12–14 December 2016; pp. 735–740. [CrossRef]
48. Semtech. LoRa Modulation Basics. 2015. Available online: http://www.semtech.com/images/datasheet/an1200.22.pdf (accessed on 25 April 2022).
49. Mroue, H.; Nasser, A.; Parrein, B.; Hamrioui, S.; Rouyer, G. Analytical and Simulation study for LoRa Modulation. In Proceedings of the 2018 25th International Conference on Telecommunications (ICT), St. Malo, France, 26–28 June 2018; pp. 655–659. [CrossRef]
50. Elshabrawy, T.; Robert, J. Interleaved chirp spreading LoRa-based modulation. *IEEE Internet Things J.* **2019**, *6*, 3855–3863. [CrossRef]
51. Abdelfadeel, K.Q.; Cionca, V.; Pesch, D. A Fair Adaptive Data Rate Algorithm for LoRaWAN. In Proceedings of the EWSN 2018, Madrid, Spain, 14–16 February 2018; pp. 1–2.
52. Iglesias-rivera, A.; Van Glabbeek, R.; Guerra, E.O.; Braeken, A.; Steenhaut, K.; Cruz-enriquez, H. Time-Slotted Spreading Factor Hopping for Mitigating Blind Spots in LoRa-Based Networks. *Sensors* **2022**, *22*, 2253. [CrossRef]
53. Liang, R.; Zhao, L.; Wang, P. Performance evaluations of lora wireless communication in building environments. *Sensors* **2020**, *20*, 3828. [CrossRef] [PubMed]
54. Chinchilla-Romero, N.; Navarro-Ortiz, J.; Muñoz, P.; Ameigeiras, P. Collision avoidance resource allocation for LoRaWAN. *Sensors* **2021**, *21*, 1218. [CrossRef]
55. Guo, Q.; Yang, F.; Wei, J. Experimental evaluation of the packet reception performance of LoRa. *Sensors* **2021**, *21*, 1071. [CrossRef]
56. Pham, C.; Ehsan, M. Dense deployment of LoRa networks: Expectations and limits of channel activity detection and capture effect for radio channel access. *Sensors* **2021**, *21*, 825. [CrossRef]
57. Spadaccino, P.; Crinó, F.G.; Cuomo, F. LoRaWAN Behaviour Analysis through Dataset Traffic Investigation. *Sensors* **2022**, *22*, 2470. [CrossRef]

58. Mullick, A.; Abd Rahman, A.H.; Dahnil, D.P.; Noraini, N.M.R. Enhancing data transmission in duct air quality monitoring using mesh network strategy for LoRa. *PeerJ Comput. Sci.* **2022**, *8*, e939. [CrossRef]
59. Onumanyi, A.J.; Abu-Mahfouz, A.M.; Hancke, G.P. Low power wide area network, cognitive radio and the internet of things: Potentials for integration. *Sensors* **2020**, *20*, 6837. [CrossRef]
60. Heeger, D.; Garigan, M.; Tsiropoulou, E.E.; Plusquellic, J. Secure LoRa firmware update with adaptive data rate techniques. *Sensors* **2021**, *21*, 2384. [CrossRef] [PubMed]
61. Gutiérrez-Gómez, A.; Rangel, V.; Edwards, R.M.; Davis, J.G.; Aquino, R.; López-De la Cruz, J.; Mendoza-Cano, O.; Lopez-Guerrero, M.; Geng, Y. A propagation study of LoRA P2P links for IoT applications: The case of near-surface measurements over semitropical rivers. *Sensors* **2021**, *21*, 6872. [CrossRef]
62. Dos Reis, B.R.; Easton, Z.; White, R.R.; Fuka, D. A LoRa sensor network for monitoring pastured livestock location and activity. *Transl. Anim. Sci.* **2021**, *5*, txab010. [CrossRef] [PubMed]
63. Van Truong, T.; Nayyar, A.; Masud, M. A novel air quality monitoring and improvement system based on wireless sensor and actuator networks using LoRa communication. *PeerJ Comput. Sci.* **2021**, *7*, e711. [CrossRef] [PubMed]
64. González, E.; Casanova-Chafer, J.; Romero, A.; Vilanova, X.; Mitrovics, J.; Llobet, E. Lora sensor network development for air quality monitoring or detecting gas leakage events. *Sensors* **2020**, *20*, 6225. [CrossRef] [PubMed]
65. Mateos Matilla, D.; Lozano Murciego, Á.; Jiménez-Bravo, D.M.; Sales Mendes, A.; Leithardt, V.R. Low-cost Edge Computing devices and novel user interfaces for monitoring pivot irrigation systems based on Internet of Things and LoRaWAN technologies. *Biosyst. Eng.* **2021**, *in press*. [CrossRef]
66. Tozer, T.C.; Withers, D.J. Satellite communications. *IEE Proc. Commun. Radar Signal Process.* **2022**, *133*, 317–318. [CrossRef]
67. Dimitrievski, A.; Filiposka, S.; Melero, F.J.; Zdravevski, E.; Lameski, P.; Pires, I.M.; Garcia, N.M.; Lousado, J.P.; Trajkovik, V. Rural healthcare IoT architecture based on low-energy LoRa. *Int. J. Environ. Res. Public Health* **2021**, *18*, 7660. [CrossRef]
68. Froiz-Míguez, I.; Lopez-Iturri, P.; Fraga-Lamas, P.; Celaya-Echarri, M.; Blanco-Novoa, Ó.; Azpilicueta, L.; Falcone, F.; Fernández-Caramés, T.M. Design, implementation, and empirical validation of an IoT smart irrigation system for fog computing applications based on Lora and Lorawan sensor nodes. *Sensors* **2020**, *20*, 6865. [CrossRef]
69. Behjati, M.; Mohd Noh, A.B.; Alobaidy, H.A.; Zulkifley, M.A.; Nordin, R.; Abdullah, N.F. Lora communications as an enabler for internet of drones towards large-scale livestock monitoring in rural farms. *Sensors* **2021**, *21*, 5044. [CrossRef] [PubMed]
70. Tseng, K.H.; Chung, M.Y.; Chen, L.H.; Chang, P.Y. Green smart campus monitoring and detection using LoRa. *Sensors* **2021**, *21*, 6582. [CrossRef] [PubMed]
71. Cruz, N.; Cota, N.; Tremoceiro, J. Lorawan and urban waste management—A trial. *Sensors* **2021**, *21*, 2142. [CrossRef] [PubMed]
72. Asiain, D.; Antolín, D. Lora-based traffic flow detection for smart-road. *Sensors* **2021**, *21*, 338. [CrossRef]
73. Pham, C. Low-cost, low-power and long-range image sensor for visual surveillance. In Proceedings of the Annual International Conference on Mobile Computing and Networking, MOBICOM, New York, NY, USA, 3–7 October 2016; pp. 35–40. [CrossRef]
74. Makkaoui, L.; Lecuire, V.; Moureaux, J.M. Fast zonal DCT-based image compression for wireless camera sensor networks. In Proceedings of the 2010 2nd International Conference on Image Processing Theory, Tools and Applications—IPTA 2010, Paris, France, 7–10 July 2010; pp. 126–129. [CrossRef]
75. Duran-Faundez, C.; Lecuire, V. Error resilient image communication with chaotic pixel interleaving for wireless camera sensors. In Proceedings of the 2008 Workshop on Real-World Wireless Sensor Networks—REALWSN 2008, Glasgow, UK, 1 April 2008; pp. 21–25. [CrossRef]
76. Ji, M.; Yoon, J.; Choo, J.; Jang, M.; Smith, A. LoRa-based Visual Monitoring Scheme for Agriculture IoT. In Proceedings of the SAS 2019—2019 IEEE Sensors Applications Symposium, Sophia Antipolis, France, 11–13 March 2019; pp. 1–6. [CrossRef]
77. Staikopoulos, A.; Kanakaris, V.; Papakostas, G.A. Image Transmission via LoRa Networks—A Survey. In Proceedings of the 2020 IEEE 5th International Conference on Image, Vision and Computing—ICIVC 2020, Beijing, China, 10–12 July 2020; pp. 150–154. [CrossRef]
78. Kirichek, R.; Pham, V.D.; Kolechkin, A.; Al-Bahri, M.; Paramonov, A. *Transfer of Multimedia Data via LoRa*; Lecture Notes in Computer Science (including subseries Lecture Notes in Artificial Intelligence and Lecture Notes in Bioinformatics); Springer: Cham, Switzerland, 2017; pp. 708–720. [CrossRef]
79. Chen, T.; Eager, D.; Makaroff, D. Efficient image transmission using lora technology in agricultural monitoring iot systems. In Proceedings of the 2019 International Conference on Internet of Things (iThings) and IEEE Green Computing and Communications (GreenCom) and IEEE Cyber, Physical and Social Computing (CPSCom) and IEEE Smart Data (SmartData), Atlanta, GA, USA, 14–17 July 2019; pp. 937–944. [CrossRef]
80. Wei, Z.; Yang, L.; Wang, Z.; Zhang, B.; Lin, Y.; Wu, Y. Wide Angle SAR Subaperture Imaging Based on Modified Compressive Sensing. *IEEE Sens. J.* **2018**, *18*, 5439–5444. [CrossRef]
81. Juliando, D.E.; Putra, R.G.; Sartika, D.A.; Yudha, R.G. Study of Lora Module Ra-02 for Long Range, Low Power, Low Rate Picture Transfer Applications. *J. Phys. Conf. Ser.* **2021**, *1845*, 012054. [CrossRef]
82. Marin, J.; Betancur, L.; Arguello, H. Modelo de Muestreo Comprimido Multiespectral para Radio Cognitiva Compressed Sensing Multiespectral Model for Cognitive Radio Networks. *Ingeniare: Revista Chilena de Ingenieria*. 2018. Available online: https://www.researchgate.net/profile/Jeison-Marin-Alfonso/publication/325838887_Modelo_de_muestreo_comprimido_multiespectral_para_radio_cognitiva/links/5e4c0fe6a6fdccd965b0a0eb/Modelo-de-muestreo-comprimido-multiespectral-para-radio-cognitiva.pdf (accessed on 24 April 2022).

83. Temim, M.A.B.; Ferre, G.; Laporte-Fauret, B.; Dallet, D.; Minger, B.; Fuche, L. An Enhanced Receiver to Decode Superposed LoRa-like Signals. *IEEE Internet Things J.* **2020**, *7*, 7419–7431. [CrossRef]
84. Romero, D.; Kim, S.J.; Giannakis, G.B. Online spectrum cartography via quantized measurements. In Proceedings of the 2015 49th Annual Conference on Information Sciences and Systems—CISS 2015, Baltimore, MD, USA, 18–20 March 2015; pp. 2–5. [CrossRef]
85. Wu, T.; Ruland, C. An Improved Authenticated Compressive Sensing Imaging. In Proceedings of the 2018 IEEE 12th International Conference on Semantic Computing (ICSC), Laguna Hills, CA, USA, 31 January–2 February 2018; pp. 164–171. [CrossRef]
86. Salomon, D. *Data Compression The Complete Reference FourthEdition*. *J. Chem. Inf. Model.* **2007**, *53*, 1689–1699. [CrossRef]
87. Walter, D. Fractal and Wavelet Image Compression of Astronomical Images. 2003. Available online: https://www.spiedigitallibrary.org/ebooks/ (accessed on 28 May 2019).
88. Donoho, D.L. Compressed sensing. *IEEE Trans. Inf. Theory* **2006**, *52*, 1289–1306. doi:10.1109/Tit.2006.871582. [CrossRef]
89. Qian, P.; Guo, Y.; Li, N.; Sun, B. Multiple target localization and power estimation in wireless sensor networks using compressive sensing. In Proceedings of the 2015 International Conference on Wireless Communications and Signal Processing—WCSP 2015, Nanjing, China, 15–17 October 2015; pp. 1–5. [CrossRef]
90. Candes, E.; Wakin, M. An Introduction To Compressive Sampling. *IEEE Signal Process. Mag.* **2008**, *25*, 21–30. [CrossRef]
91. Jayawickrama, B.A.; Dutkiewicz, E.; Fang, G.; Oppermann, I.; Mueck, M. Downlink power allocation algorithm for licence-exempt LTE systems using Kriging and Compressive Sensing based spectrum cartography. In Proceedings of the GLOBECOM—IEEE Global Telecommunications Conference, Atlanta, GA, USA, 9–13 December 2013; pp. 3766–3771. [CrossRef]
92. Naghsh, N.; Ghorbani, A.; Amindavar, H. Compressive sensing for microwave breast cancer imaging. *IET Signal Process.* **2018**, *12*, 242–246. [CrossRef]
93. Marín, A.J.; Martinez, T.J.I.; Betancur, L.; Arguello, H. *Compressive Multispectral Model for Spectrum Sensing in Cognitive Radio Networks*; IEEE: Kos, Greece, 2017; pp. 2640–2644, ISBN 9780992862671.
94. Ramdani, S.; Basari. Compressive sensing approach for microwave imaging application. In Proceedings of the 2018 International Conference on Signals and Systems—ICSigSys 2018, Bali, Indonesia, 1–3 May 2018; pp. 197–200. [CrossRef]
95. Saupe, D.; Hamzaoui, R.; Hartenstein, H. Fractal Image Compression An Introductory Overview. 2006, p. 66. Available online: https://karczmarczuk.users.greyc.fr/matrs/Dess/RADI/Refs/SaHaHa96a.pdf (accessed on 24 April 2022).
96. Kim, S.J.; Dall'Anese, E.; Giannakis, G.B. Cooperative Spectrum Sensing for Cognitive Radios Using Kriged Kalman Filtering. *IEEE J. Sel. Top. Signal Process.* **2011**, *5*, 24–36. [CrossRef]
97. Kim, S.j.; Jain, N.; Giannakis, G.B.; Forero, P.A. Joint Link Learning and Cognitive Radio Sensing. In Proceedings of the 2011 Conference Record of the Forty Fifth Asilomar Conference on Signals, Systems and Computers (ASILOMAR), Pacific Grove, CA, USA, 6–9 November 2011; pp. 1415–1419.
98. Marini, R.; Mikhaylov, K.; Pasolini, G.; Buratti, C. Lorawansim: A flexible simulator for lorawan networks. *Sensors* **2021**, *21*, 695. [CrossRef] [PubMed]
99. Bankov, D.; Khorov, E.; Lyakhov, A. On the Limits of LoRaWAN Channel Access. In Proceedings of the 2016 International Conference on Engineering and Telecommunication, Moscow, Russia, 29–30 November 2016; pp. 10–14. [CrossRef]
100. Ali, A.; Shah, G.A.; Farooq, M.O.; Ghani, U. Technologies and challenges in developing Machine-to-Machine applications: A survey. *J. Netw. Comput. Appl.* **2017**, *83*, 124–139. [CrossRef]
101. Raza, U.; Kulkarni, P.; Sooriyabandara, M. Low Power Wide Area Networks: An Overview. *IEEE Commun. Surv. Tutor.* **2017**, *19*, 855–873. [CrossRef]
102. Feng, C.; Valaee, S.; Tan, Z. Multiple target localization using compressive sensing. In Proceedings of the GLOBECOM—IEEE Global Telecommunications Conference, Honolulu, HI, USA, 30 November–4 December 2009. [CrossRef]
103. Tropp, J.a.; Gilbert, A.C. Via Orthogonal Matching Pursuit. *IEEE Trans. Inf. Theory* **2007**, *53*, 4655–4666. [CrossRef]
104. Jayawickrama, B.A.; Dutkiewicz, E.; Oppermann, I.; Fang, G.; Ding, J. Improved performance of spectrum cartography based on compressive sensing in cognitive radio networks. In Proceedings of the 2013 IEEE International Conference on Communications (ICC), Budapest, Hungary, 9–13 June 2013; pp. 5657–5661. [CrossRef]
105. Jamali-Rad, H.; Ramezani, H.; Leus, G. Sparse multi-target localization using cooperative access points. In Proceedings of the IEEE Sensor Array and Multichannel Signal Processing Workshop, Hoboken, NJ, USA, 17–20 June 2012; pp. 353–356. [CrossRef]
106. Krishnan, B.S.; Vaze, R.; Manjunath, D. On white-space detection, localization and coverage. In Proceedings of the 2014 20th National Conference on Communications—NCC 2014, Kanpur, Uttar Pradesh, India, 28 February–2 March 2014. [CrossRef]
107. Thomos, N.; Boulgouris, N.V.; Strintzis, M.G. Optimized transmission of JPEG2000 streams over wireless channels. *IEEE Trans. Image Process.* **2006**, *15*, 54–67. [CrossRef]
108. Li, L.; Ren, J.; Zhu, Q. On the Application of LoRa LPWAN Technology in Sailing Monitoring System. In Proceedings of the 2017 13th Annual Conference on Wireless On-demand Network Systems and Services (WONS), Jackson, WY, USA, 21–24 February 2017; pp. 77–80. [CrossRef]